Table 4. Continued.

Probe sets	medulla/ papilla	cortex/ papilla	medulla/ cortex	GENE_SYMBOL	GENE_NAME	channel transporter	Metabolic enzymes	cytoskeleton /extracellular matrix
1387941_s_at	16.1	14.6	1.1	Pla2g6	phospholipase A2, group VI			
1372750_at	3.7	0.2	15.9	Fst	Follistatin			
1370072_at	15.6	12.1	1.3	Mme	membrane metallo endopeptidase			
1387966_at	15.5	11.4	1.4	Asrgl1	asparaginase-like sperm autoantigen			
1384831_at	15.1	11.7	1.3	Slc7a13_predicted	solute carrier family 7, (cationic amino acid transporter, y+ system) member 13 (predicted)			
1368189_at	14.8	11.3	1.3	Dhcr7	7-dehydrocholesterol reductase			
1367798_at	14.5	11.2	1.3	Ahcy	S-adenosylhomocysteine hydrolase			
1371059_at	14.5	14.4	1.0	Prkar2a	protein kinase, cAMP-dependent, regulatory, type 2, alpha			
1369158_at	14.4	14.3	1.0	Casr	calcium-sensing receptor			
1370030_at	14.1	11.5	1.2	Gclm	glutamate cysteine ligase, modifier subunit			
1398350_at	14.0	12.9	1.1	Basp1	brain abundant, membrane attached signal protein 1			
1369728_at	13.7	10.7	1.3	Hist1h4m_predicted	histone 1, H4m (predicted)			
1387223_at	13.6	12.2	1.1	Aadat	aminoadipate aminotransferase			
1370529_a_at	12.8	7.7	1.7	Pld1	phospholipase D1			
1384603_at	12.8	9.8	1.3	Abca4_predicted	ATP-binding cassette, sub-family A (ABC1), member 4 (predicted)			
1369494_a_at	12.0	6.6	1.8	Ghrhr	growth hormone releasing hormone receptor			
1367729_at	11.9	11.4	1.0	Oat	ornithine aminotransferase			
1374565_at	11.8	9.7	1.2	Nek6	NIMA (never in mitosis gene a)-related expressed kinase 6			
1368431_at	11.6	10.3	1.1	Hpn	hepsin			
1382274_at	11.5	5.5	2.1	Rarres1_predicted	retinoic acid receptor responder (tazarotene induced) 1 (predicted)			
1374871_at	11.2	7.3	1.5	Asrgl1	asparaginase-like sperm autoantigen			
1392965_a_at	11.0	2.3	4.8	Smoc2_predicted	SPARC related modular calcium binding 2 (predicted)			
1370163_at	11.0	6.5	1.7	Odc1	ornithine decarboxylase 1			
1390208_at	10.7	10.7	1.0	Htatip2_predicted	HIV-1 Tat interactive protein 2 (predicted)			
1370530_a_at	10.6	5.7	1.9	Pld1	phospholipase D1			
1376852_at	10.5	8.3	1.3	Mccc1_predicted	methylcrotonoyl-Coenzyme A carboxylase 1 (alpha) (predicted)			
1369184_at	10.5	6.8	1.5	Cldn16	claudin 16			
1385970_at	10.4	9.5	1.1	Sh2bp1_predicted	SH2 domain binding protein 1 (tetratricopeptide repeat containing) (predicted)			
1383742_at	10.1	9.4	1.1	Snx7_predicted	sorting nexin 7 (predicted)			

After selection by ANOVA ($p<0.01$) for the data of percellome normalization, genes maximally expressed in medulla were selected. The genes were aligned in the order of the ratio to the lower expression value, either in papilla or in cortex. As the genes listed here are expressed in medulla and cortex to a similar extent, exceptional cases (ratio >3) are shaded in the medulla/cortex column. The genes categorized to "channel/transporters", "metabolic enzymes", or "cytoskeleton/extracellular matrix" are also shaded. Proteases or enzymes involving signal transduction are not included in the category of "metabolic enzymes". For simplicity, genes with less than 10-fold specificity are omitted.

Table 5. A list of probe sets specifically expressed in cortex of kidney.

Probe sets	cortex/ papilla	medulla/ papilla	cortex/ medulla	GENE_SYMBOL	GENE_NAME	channel transporter	Metabolic enzymes	cytoskeleton /extracellular matrix
1387314_at	312.0	259.8	1.2	Sult1b1	sulfotransferase family 1B, member 1			
1387820_at	284.9	14.7	19.4	Klk7	kallikrein 7			
1388172_at	245.4	110.3	2.2	Ust1r	integral membrane transport UST1r			
1368064_a_at	230.1	19.6	11.8	Ddc	dopa decarboxylase			
1390591_at	224.2	166.1	1.3	Slc17a3	Na/Pi cotransporter 4			
1368467_at	217.1	117.6	1.8	Cyp4f2	cytochrome P450, family 4, subfamily F, polypeptide 2			
1368600_at	210.7	75.0	2.8	Slc26a1	solute carrier family 26 (sulfate transporter), member 1			
1396039_at	202.5	188.6	1.1	Slc22a12_predicted	solute carrier family 22 (organic anion/cation transporter), member 12 (predicted)			
1387230_at	193.9	13.2	14.7	Slc12a3	solute carrier family 12, member 3			
1368245_at	192.4	134.7	1.4	Upb1	ureidopropionase, beta			
1367917_at	192.3	124.6	1.5	Cyp2d26	cytochrome P450, family 2, subfamily d, polypeptide 26			
1367871_at	187.8	32.3	5.8	Cyp2e1	cytochrome P450, family 2, subfamily e, polypeptide 1			
1376267_at	185.1	13.9	13.4	Slc16a6	Solute carrier family 16 (monocarboxylic acid transporters), member 6			
1384877_at	183.4	73.9	2.5	Aqp11	aquaporin 11			
1398282_at	174.5	75.2	2.3	Kynu	kynureninase (L-kynurenine hydrolase)			
1370547_at	169.5	56.4	3.0	Pzp	pregnancy-zone protein			
1368563_at	149.7	96.7	1.5	Aspa	aspartoacylase			
1383111_at	149.3	60.1	2.5	Acmsd	2-amino-3-carboxymuconate-6-semialdehyde decarboxylase			
1370991_at	146.7	32.6	4.5	Cml3	camello-like 3			
1387188_at	144.5	86.8	1.7	RGD:620099	solute carrier family 17 (sodium phosphate), member 1			
1370936_at	143.4	91.3	1.6	Dmgdh	dimethylglycine dehydrogenase precursor			
1367804_at	142.8	21.8	6.5	Sap	serum amyloid P-component			
1368915_at	141.5	87.2	1.6	Kmo	kynurenine 3-monooxygenase (kynurenine 3-hydroxylase)			
1398511_at	138.7	16.8	8.3	Susd2_predicted	sushi domain containing 2 (predicted)			
1387851_at	129.9	78.3	1.7	Pter	phosphotriesterase related			
1376051_at	127.0	63.2	2.0	Cryl1	crystallin, lamda 1			
1384112_at	125.1	80.6	1.6	Nt5	5 nucleotidase			
1393894_at	123.8	94.1	1.3	RGD:628846	cytochrome P450, 4a12			
1370725_a_at	116.9	15.4	7.6	G6pc	glucose-6-phosphatase, catalytic			
1386980_at	116.6	64.2	1.8	Apom	apolipoprotein M			
1377125_at	116.3	28.0	4.2	Dnajc6_predicted	DnaJ (Hsp40) homolog, subfamily C, member 6 (predicted)			
1368317_at	114.8	70.5	1.6	Aqp7	aquaporin 7			
1370615_at	114.4	28.0	4.1	RGD:708417	UDP-glucuronosyltransferase			

Table 5. Continued.

Probe sets	cortex/ papilla	medulla/ papilla	cortex/ medulla	GENE_SYMBOL	GENE_NAME	channel transporter	Metabolic enzymes	cytoskeleton /extracellular matrix
1368236_at	113.4	105.5	1.1	Mep1a	meprin 1 alpha			
1373386_at	113.2	110.8	1.0	Gjb2	gap junction membrane channel protein beta 2			
1369636_at	112.6	41.2	2.7	Sord	sorbitol dehydrogenase			
1368521_at	110.8	46.3	2.4	Napsa	napsin A aspartic peptidase			
1368150_at	110.4	78.2	1.4	Slc27a2 /// LOC497779	solute carrier family 27 (fatty acid transporter), member 2 /// hypothetical gene supported by NM_031736			
1369635_at	109.5	42.4	2.6	Sord	sorbitol dehydrogenase			
1368180_s_at	107.9	73.9	1.5	Gsta2	glutathione-S-transferase, alpha type2			
1368190_at	105.6	12.1	8.7	Ren1	renin 1			
1377051_at	104.7	17.9	5.8	Mpv17l_predicted	Mpv17 transgene, kidney disease mutant-like (predicted)			
1387336_at	102.7	89.7	1.1	Nat8	*N*-acetyltransferase 8 (camello like)			
1387631_at	102.4	59.8	1.7	Hpgd	15-hydroxyprostaglandin dehydrogenase			
1379885_at	100.7	91.4	1.1	Fmo4	flavin containing monooxygenase 4			
1368659_at	100.0	60.0	1.7	Agxt2	alanine-glyoxylate aminotransferase 2			
1370259_a_at	99.6	31.1	3.2	Pthr1	parathyroid hormone receptor 1			
1368188_at	94.6	25.6	3.7	Hpd	4-hydroxyphenylpyruvic acid dioxygenase			
1369200_at	93.4	56.3	1.7	Nt5	5 nucleotidase			
1387053_at	90.3	37.7	2.4	Fmo1	flavin containing monooxygenase 1			
1388569_at	88.3	50.7	1.7	Serpinf1	serine (or cysteine) proteinase inhibitor, clade F), member 1			
1390857_at	87.5	26.6	3.3	Xylb_predicted	xylulokinase homolog (H. influenzae) (predicted)			
1387375_at	86.9	64.4	1.4	Khk	ketohexokinase			
1387034_at	86.3	17.7	4.9	Pah	phenylalanine hydroxylase			
1397740_at	86.3	51.0	1.7	Sfxn1_predicted	sideroflexin 1 (predicted)			
1368736_at	84.2	18.9	4.4	Tsx	testis specific X-linked gene			
1398514_at	82.6	81.3	1.0	Hgd_predicted	homogentisate 1, 2-dioxygenase (predicted)			
1368515_at	81.1	7.2	11.3	Epb4.1l3	erythrocyte protein band 4.1-like 3			
1368794_at	81.0	78.4	1.0	Haao	3-hydroxyanthranilate 3,4-dioxygenase			
1370964_at	80.8	27.0	3.0	Ass	arginosuccinate synthetase			
1368077_at	79.6	43.0	1.9	Fbp1	fructose-1,6- biphosphatase 1			
1370397_at	77.6	68.8	1.1	Cyp4a14	cytochrome P450, family 4, subfamily a, polypeptide 14			
1368397_at	76.3	36.6	2.1	Ugt2b5 /// Ugt2b4	UDP-glucuronosyltransferase 2 family, member 5 /// UDP glycosyltransferase 2 family, polypeptide B4			
1368282_at	74.3	24.9	3.0	Dpep1	dipeptidase 1 (renal)			
1395026_at	73.7	59.0	1.2	Fmo4	flavin containing monooxygenase 4			
1380577_at	70.1	53.6	1.3	Abcg2	ATP-binding cassette, sub-family G (WHITE), member 2			

Table 5. Continued.

Probe sets	cortex/ papilla	medulla/ papilla	cortex/ medulla	GENE_SYMBOL	GENE_NAME	channel transporter	Metabolic enzymes	cytoskeleton /extracellular matrix
1387339_at	69.4	19.2	3.6	Sepp1	selenoprotein P, plasma, 1			
1382913_at	68.9	16.8	4.1	Cttnbp2	cortactin binding protein 2			
1376327_at	68.9	24.2	2.8	Tnfrsf14_predicted	tumor necrosis factor receptor superfamily, member 14 (herpesvirus entry mediator) (predicted)			
1368178_at	66.6	32.4	2.1	Pdzk1	PDZ domain containing 1			
1377672_at	66.3	37.3	1.8	Sult1c2	sulfotransferase family, cytosolic, 1C, member 2			
1387084_at	65.5	55.5	1.2	Dpp4	dipeptidylpeptidase 4			
1374512_at	63.7	35.5	1.8	Cdh7	Cadherin 7, type 2			
1371824_at	63.6	40.8	1.6	Ak3l1	adenylate kinase 3-like 1			
1369412_a_at	63.4	37.9	1.7	Slc19a1	solute carrier family 19, member 1			
1373803_a_at	63.1	39.2	1.6	Ghr	growth hormone receptor			
1387259_at	62.9	29.4	2.1	Cdh2 /// LOC497718	cadherin 2 /// hypothetical gene supported by NM_031333			
1389166_at	62.8	31.1	2.0	Cib2_predicted	calcium and integrin binding family member 2 (predicted)			
1371354_at	62.1	8.0	7.8	Tncc_predicted	troponin C, cardiac/slow skeletal (predicted)			
1372672_at	58.8	36.8	1.6	Qprt_predicted	quinolinate phosphoribosyltransferase (predicted)			
1369491_at	58.4	36.1	1.6	Dao1	D-amino acid oxidase			
1387111_at	57.3	33.4	1.7	Ddah1	dimethylarginine dimethylaminohydrolase 1			
1367988_at	57.1	22.1	2.6	Cyp2c23	cytochrome P450, family 2, subfamily c, polypeptide 23			
1368607_at	56.5	51.1	1.1	RGD:628846	cytochrome P450, 4a12			
1370881_at	55.8	22.9	2.4	Tst	thiosulfate sulfurtransferase			
1369259_at	55.6	28.4	2.0	Dio1	deiodinase, iodothyronine, type I			
1376709_at	55.2	42.5	1.3	Slc39a8_predicted	solute carrier family 39 (metal ion transporter), member 8 (predicted)			
1387013_at	55.2	27.3	2.0	Tmem27	kidney-specific membrane protein			
1387808_at	54.9	5.1	10.8	Slc7a7	solute carrier family 7 (cationic amino acid transporter, y+ system), member 7			
1368283_at	54.7	29.8	1.8	Ehhadh	enoyl-Coenzyme A, hydratase/3-hydroxyacyl Coenzyme A dehydrogenase			
1373337_at	53.4	22.5	2.4	Grhpr_predicted	glyoxylate reductase/hydroxypyruvate reductase (predicted)			
1383654_a_at	53.2	14.7	3.6	Fnsk	similar to fructosamine-3-kinase			
1368924_at	51.8	42.4	1.2	Ghr	growth hormone receptor			
1368092_at	50.7	35.9	1.4	Fah	fumarylacetoacetate hydrolase			
1380171_at	49.4	39.5	1.3	Adra2b	Adrenergic receptor, alpha 2b			
1367952_at	45.8	26.5	1.7	Lrp2	low density lipoprotein receptor-related protein 2			

Table 5. Continued.

Probe sets	cortex/ papilla	medulla/ papilla	cortex/ medulla	GENE_SYMBOL	GENE_NAME	channel transporter	Metabolic enzymes	cytoskeleton /extracellular matrix
1369705_at	44.1	42.6	1.0	RGD:621651	X transporter protein 3			
1368680_a_at	43.6	25.3	1.7	Slc34a1	solute carrier family 34 (sodium phosphate), member 1			
1367627_at	43.5	14.8	2.9	Gatm	glycine amidinotransferase (L-arginine:glycine amidinotransferase)			
1379950_at	42.9	37.7	1.1	Cml2	Camello-like 2			
1367775_at	42.6	32.3	1.3	Amacr	alpha-methylacyl-CoA racemase			
1388176_at	42.4	24.0	1.8	Cml5	camello-like 5			
1368322_at	42.1	8.2	5.1	Sod3	superoxide dismutase 3, extracellular			
1372264_at	42.1	15.9	2.7	Pck1	phosphoenolpyruvate carboxykinase 1			
1397647_at	41.9	17.1	2.5	Slc25a15_predicted	solute carrier family 25 (mitochondrial carrier; ornithine transporter) member 15 (predicted)			
1369073_at	41.9	12.2	3.4	Nr1h4	nuclear receptor subfamily 1, group H, member 4			
1368877_at	41.6	13.7	3.0	Znf354a	zinc finger protein 354A			
1390119_at	41.4	4.9	8.4	Sfrp2	secreted frizzled-related protein 2			
1367774_at	41.1	31.8	1.3	Gsta5	glutathione S-transferase A5			
1376191_at	40.1	27.6	1.5	Hpgd	15-hydroxyprostaglandin dehydrogenase			
1397526_at	39.3	23.5	1.7	Gcdh_predicted	glutaryl-Coenzyme A dehydrogenase (predicted)			
1374384_at	38.8	16.3	2.4	Crygc	Crystallin, gamma C			
1387491_at	38.5	10.9	3.5	Gyk	glycerol kinase			
1386944_a_at	38.3	7.7	5.0	G6pc	glucose-6-phosphatase, catalytic			
1367999_at	37.7	22.6	1.7	Aldh2	aldehyde dehydrogenase 2			
1369182_at	37.6	9.6	3.9	F3	coagulation factor 3			
1382975_at	37.4	20.8	1.8	Ceacam1	CEA-related cell adhesion molecule 1			
1374200_at	36.1	16.7	2.2	Slc29a3	solute carrier family 29 (nucleoside transporters), member 3			
1369973_at	35.6	9.6	3.7	Xdh /// LOC497811	xanthine dehydrogenase /// hypothetical gene supported by NM_017154			
1372306_at	35.4	22.9	1.5	Ethe1_predicted	ethylmalonic encephalopathy 1 (predicted)			
1370818_at	34.6	12.5	2.8	Decr2	2-4-dienoyl-Coenzyme A reductase 2, peroxisomal			
1397797_at	33.3	29.3	1.1	Tigd3	Tigger transposable element derived 3 (predicted)			
1372323_at	32.9	23.4	1.4	Sardh	sarcosine dehydrogenase			
1368412_a_at	32.5	5.3	6.1	Ptpro	protein tyrosine phosphatase, receptor type, O			
1390036_at	32.5	6.0	5.4	Slc16a6	solute carrier family 16 (monocarboxylic acid transporters), member 6			
1397744_at	32.5	22.2	1.5	Sardh	Sarcosine dehydrogenase			
1368642_at	32.4	19.5	1.7	Cdh2 /// LOC497718	cadherin 2 /// hypothetical gene supported by NM_031333			
1373188_at	32.0	12.2	2.6	Scn4b	sodium channel, voltage-gated, type IV, beta			

Table 5. Continued.

Probe sets	cortex/ papilla	medulla/ papilla	cortex/ medulla	GENE_SYMBOL	GENE_NAME	channel transporter	Metabolic enzymes	cytoskeleton /extracellular matrix
1373667_at	31.8	14.0	2.3	Ccbl1_predicted	cysteine conjugate-beta lyase (predicted)			
1372031_at	31.7	7.5	4.2	Dab2	Disabled homolog 2 (Drosophila)			
1390585_at	31.7	10.9	2.9	Masp1	mannan-binding lectin serine peptidase 1			
1386981_at	31.6	3.7	8.4	Slc16a1	solute carrier family 16 (monocarboxylic acid transporters), member 1			
1368253_at	31.5	28.7	1.1	Gamt	guanidinoacetate methyltransferase			
1388537_at	31.4	15.2	2.1	Nipsnap1_predicted	4-nitrophenylphosphatase domain and non-neuronal SNAP25-like protein homolog 1 (C. elegans) (predicted)			
1387165_at	31.1	4.4	7.1	Maf	v-maf musculoaponeurotic fibrosarcoma (avian) oncogene homolog (c-maf)			
1384273_at	30.9	10.2	3.0	Carkl_predicted	carbohydrate kinase-like (predicted)			
1380393_at	30.9	30.7	1.0	Cryz_predicted	crystallin, zeta (predicted)			
1393947_at	30.7	12.7	2.4	Slc25a15_predicted	solute carrier family 25 (mitochondrial carrier; ornithine transporter) member 15 (predicted)			
1378197_at	30.4	9.5	3.2	KIFC2	kinesin family member C2			
1379582_a_at	30.1	14.5	2.1	Ccna2	cyclin A2			
1382434_at	30.0	23.5	1.3	Entpd5	ectonucleoside triphosphate diphosphohydrolase 5			

After selection by ANOVA ($p<0.01$) for the data of percellome normalization, genes maximally expressed in cortex were selected. The genes were aligned in the order of the ratio to the lower expression value, either in papilla or in medulla. Among the genes listed here, relatively specific ones for cortex (ratio>3) are shaded in the cortex/medulla column. The genes categorized to "channel/transporters", "metabolic enzymes", or "cytoskeleton/extracellular matrix" are also shaded. Proteases or enzymes involving signal transduction are not included in the category of "metabolic enzymes". For simplicity, genes with less than 30-fold specificity are omitted.

Table 6. Regionally specific genes in rat kidney.

	Channel/transporter	Metabolizing enzymes	Cytoskeleton/ extracellular matrix	Others of interest
Papilla	Slco4a1, Aqp3, Aqp4, Fxyd4, Slc4a11, Clcnk1, bsnd	Ptgs1, Ptgs2, Aldh1a3, Akr1b4, Ugt8, Ltb4dh	Capg, Plekhb1, Coll8a1, Spnb3, Hs3st1, Krt1-18	Hspa2, Hspa1a, Hspb1
Medulla	Scl21a1, Scl21a13, Slc23a3, Slc21a9, UST5r, Scl6a18, Scl38a3, Slc22a2, Slc7a12, Slc15a2	CYP2d9, CYP2c, Hnmt, Pklr, Fmo3, Dhrs7, Akr1c12, Gclc, Ggt1, Tmlhe		Prlr, Ace2
Cortex	Ust1r, Slc17a3, Slc26a1, Slc22a12, Slc12a3, Slc16a6, Aqp11, Aqp7, Gjb2, Slc27a2	Sult1b1, Klk7, Ddc, CYP2d26, CYP2e1, CYP4f2, Upb1, Aspa, Acmsd, Dmgdh, Kmo		Ren1

Genes categorized in channel/transporter, metabolizing enzyme and cytoskeleton/extracellular matrix from high rank in Tables 3, 4, 5 are summarized by using gene symbols which can be referred to in the preceding tables. Interesting genes discussed in the text are included as "others".

aminoglycoside causes necrosis mainly in the proximal tubules, while puromycin does the same on glomerulus (Schnellmann, 2001). In an organ with such a complex structure, analysis by GeneChip would give different results when it is done as a whole or separated into portions. When the potential nephrotoxicity of candidate chemicals is assessed using toxicogenomics technology, it would be ideal to perform GeneChip analysis for each portion. However, it is sometimes difficult in the usual toxicity tests to obtain enough sample material for toxicogenomics analysis after sampling for other histopathological and biochemical analyses. Furthermore, it is difficult to determine which portion is to be examined when the target region of the test drug is unknown. Analyzing all of the separated portions is impractical considering the cost.

In the present study, comparison of the gene expression profile was made among each portion, papilla, medulla, and cortex, as well as between the whole slice and each portion. Although various genes or proteins with region-specific expression have been reported, their localization was toward glomerulus, distal/proximal tubules, or collecting duct, i.e., tissues from specific cell types, not the anatomical location. This way is of course desirable for cell physiological study, but is inconvenient when a potential bias in the gene expression analysis based on the position of sampling is concerned, and reports focusing on this point are scarce. It can be generally said that papilla is enriched in collecting duct and relatively scarce in glomerulus, but their proportion varies with the sampling.

When comparison between each portion was made by correlation coefficient, the correlation was decreased between the portions compared to within the same portion. The correlation of gene expression profile between cortex and medulla was relatively high, whereas that between papilla and cortex or medulla was low. Based on the correlation of each portion to the whole slice, it was concluded that gene expression in the whole slice largely reflected that of cortex, followed by medulla. The main reason is that the volume of the portion comprising the whole slice is in this order: cortex > medulla > papilla (Fig. 1). If the production of mRNA per cell is constant throughout the portions, the region-specific gene can be extracted by global normalization. However, this was found to be inappropriate.

To extract region-specific genes, detection call (absent, present, and marginal) included in the GeneChip data was utilized, i.e., genes with present call in a particular region but absent call in all others were extracted, and they were checked as to whether they had present call in the whole slice. The important point of this result is that the majority (94%) of genes specifically expressed in papilla are not detectable in the whole slice. This is consistent with the result of the correlation coefficient. It is thus concluded that the expression changes of such genes occurring in papilla cannot be detected when they are decreased, and it is difficult to measure when they are increased, but their extent is not so large, as in the analysis of the whole slice. Attention should be paid when these genes are used for the marker genes in the toxicogenomics of kidney.

As obvious from Figs. 3 and 4, global normalization of the data leads to an incorrect result in the comparison among different regions. This might be due to the fact that the transcriptional activity in papilla is much less than that in the others, and subsequently the expression of each gene in papilla was over-estimated by the normalization, using a low value. This does not mean that the global normalization is useless when drug effects are tested on the samples separated into different portions. As global normalization gives relative values to the total mRNA amount, it efficiently reveals the drug effect unless the drug brings about a large change in the total mRNA. In the present case, it became problematic simply because the comparison was made among tissues with largely different mRNA contents. An alternative way is to normalize each gene by a house-keeping gene, e.g., β-actin or GAPDH. However, as already shown above, there is no guarantee that expression of these genes is constant throughout the different tissues.

Based on the data normalized by the percellome procedure, genes with region-specific expression were extracted and aligned in the order of their relative specificity. It was then found that the majority of genes with high region-specificity were related to channel/transporter and metabolic enzyme, suggesting a good correlation between gene expression and physiological function.

There are many known members of the solute carrier family (slc), whose distribution showed an interesting and marked difference among the three portions. In papilla, slc4a family members (anion transporter) were specifically expressed. In medulla, the expression of slc21a family (organic anion transporting polypeptides; OATPs), was outstanding. There were also other members such as Slc23a3 (xanthine/uracil permease), Scl6a18 (monocarboxylic acid trans-

porter), Scl38a3 (SNAT family; Gu *et al.*, 2005), Slc22a2 (organic cation transporter), Slc7a12 (cationic amino acid transporter), and Slc15a2 (H+/peptide transporter), which were specifically expressed. In cortex, Slc17a (Na-phosphate co-transporter), Slc22a12 and Slc12a3 (both anion transporters), Slc16a6 (monocarboxylic acid transporter), and Slc27a2 (fatty acid transporter) were found to be specific.

There have been some reports regarding region-specific transporters. As glucose transport is known to be operational in the proximal tubule, it is expected that glucose transporters are enriched in cortex and medulla compared with papilla. Among the genes judged as significant by ANOVA, slc2a4 and 2a13 were glucose transporters and their expression was about 3.5-fold higher in medulla and cortex compared with papilla (this number was not large enough to be shown in the tables). It is also known that slc14a2, involved in urea transport, is highly expressed in the collecting duct (Karakashian *et al.*, 1999). Although the ratio was not large enough to be in Table 3, its expression in papilla was twofold compared with cortex, consistent with the literature.

Aquaporin (Aqp) 3 and 4 were specifically expressed in papilla while Aqp 7 and 11 were in cortex (Table 6). Although the ratio was not large enough to be in Table 3, Aqp 2 was also preferentially expressed in papilla (1.9 and 2.3 fold compared with medulla and cortex, respectively). There have been supportive reports that Aqp2 (Jo *et al.*, 1997) and Aqp3 (Echevarria *et al.*, 1994) are enriched in collecting duct and Aqp7 is highly expressed in cortex (Nejsum *et al.*, 2000).

Kidney produces renin to control blood pressure. Renin is synthesized in juxtaglomerular cells and converts angiotensinogen to angiotensin I, which is further converted to angiotensin II by angiotensin converting enzyme (ACE). The renin gene (Ren1) was expressed highest in cortex while ACE (ace2) was highest in medulla (Table 6).

Probes for prolactin receptor are 4 sets on the chip and all of them showed quite low expression in papilla (expression ranged 60 - 90 fold in cortex and 70 - 130 fold in medulla, compared with papilla, for these 4 probe sets). Prolactin is known as a natriuretic hormone which interacts with the renal dopamine system, and its natriuretic response is associated with inhibition of proximal tubular Na,K-ATPase (Ibarra *et al.*, 2005). The location of its receptor in kidney (enriched in medulla and cortex) elucidated in the present study was consistent with the region where the hormone works.

NSAID-induced nephrotoxicity is well known as a typical toxicity toward kidney (Schnellmann, 2001). Its mechanism is believed to be inhibition of cyclooxygenase (COX). COX-1 is a constitutive, house-keeping enzyme and reported to be much present in the collecting duct. COX-2 is an inducible enzyme involved in the inflammatory process, while it is reported to be always present at a low level in kidney without inflammation (Harris *et al.*, 1994). The genes for these enzymes (ptgs1 and ptgs2) were both highest in papilla. Moreover, phospholipase A2 IVA was also highest in papilla. These observations are consistent with previous reports and might be related to the fact that nephrotoxicity by NSAID is frequently associated with necrosis in papilla (Schnellmann, 2001).

On the other hand, other prostaglandin-related genes were uniformly low in papilla. The expression of the gene of 15-hydroxyprostaglandin dehydrogenase (Hpgd), which is involved in prostaglandin metabolism, was 60 and 102 fold in medulla and cortex, respectively, compared with papilla. Other prostaglandin-related genes without large enough specificity for the table were prostaglandin D2 synthase (Ptgds), prostaglandin E receptor 1 (Ptger1), prostaglandin E receptor 3 (Ptger3), and prostaglandin E receptor 4 (Ptger4), which were 6- and 26-fold, 3- and 4-fold, 5- and 2-fold, 3- and 6-fold, in medulla and cortex, respectively, compared with papilla. The expression of prostaglandin E synthase (Ptges) was exceptionally the same in papilla and medulla, and 4.5-fold of these was found in cortex.

Kallikrein that produces bradykinin is biosynthesized in kidney cortex (Xiong *et al.*, 1989). Kallikrein 7 (Klk7) is found in Table 5 showing 15-fold and 285-fold expression in medulla and cortex, respectively, compared with papilla. This is again consistent with the anatomical feature.

One unique point in the tables is that genes related to cytoskeletal proteins and heat shock proteins (both HSP70 and HSP27) selectively expressed high in papilla (Table 3 and 6). If the analysis was done by global normalization, it could be that the relative expression of these genes was apparently overestimated because of the low expression of other gene populations, such as transporters or enzymes. However, the present analysis was based on percellome normalization, and the values are directly related to the copy numbers per cell (or DNA). Therefore, enrichment of these genes means that the copy numbers of these genes are actually high. The potential involvement of

HSP70 in nephrotoxicity has been investigated in relation to renal cell survival and apoptosis, and the relationship between hsp27 and cytoskeletal proteins has also been discussed in relation to renal injury after ischemia-reperfusion (van de Water, 2006). Its pathophysiological meaning is presently unclear, especially because data of modulation by nephrotoxicants is not available, so this point is quite interesting as a future study.

In summary, many of the genes related to kidney functions showed region-related differences in their expression and some of them were consistent with previous reports. There are also many genes with unique region-related differences in the table, which have not been described in the literature and it would be worthwhile to start new investigations based on these data. In the present study, analysis of gene expression was exclusively done in non-treated animals. It is of course important to investigate the regional difference in the responsiveness to drugs, and it should be the highest priority of future study. In conclusion, comprehensive comparison data of gene expression in the renal anatomical areas would greatly enhance studies of physiological function and mechanism of toxicity in kidney.

ACKNOWLEDGMENT

This study was supported in part by a grant from the Ministry of Health, Labor and Welfare (H14-Tox-ico-001).

REFERENCES

Echevarria, M., Windhager, E.E., Tate, S.S. and Frindt, G. (1994): Cloning and expression of AQP3, a water channel from the medullary collecting duct of rat kidney. Proc. Natl. Acad. Sci. USA, **91**, 10997-11001.

Gu, S., Villegas, C.J. and Jiang, J.X. (2005): Differential Regulation of Amino Acid Transporter SNAT3 by Insulin in Hepatocytes. J. Biol. Chem., **280**, 26055-26062.

Harris, R.C., McKanna, J.A., Akai, Y., Jacobson, H.R., Dubois, R.N. and Breyer, M.D. (1994): Cyclooxygenase-2 is associated with the macula densa of rat kidney and increases with salt restriction. J. Clin. Invest., **94**, 2504-2510.

Ibarra, F., Crambert, S., Eklof, A.C., Lundquist, A., Hansell, P. and Holtback, U. (2005): Prolactin, a natriuretic hormone, interacting with the renal dopamine system. Kidney Int., **68**, 1700-1707.

Jo, I., Nielsen, S. and Harris, H.W. (1997): The 17 kDa band identified by multiple anti-aquaporin 2 antisera in rat kidney medulla is a histone. Biochim. Biophys. Acta., **1324**, 91-101.

Kanno, J., Aisaki, K., Igarashi, K., Nakatsu, N., Ono, A., Kodama, Y. and Nagao, T. (2006): "Per cell" normalization method for mRNA measurement by quantitative PCR and microarrays. BMC Genomics, **7**, 64.

Karakashian, A., Timmer, R.T., Klein, J.D., Gunn, R.B., Sands, J.M. and Bagnasco, S.M. (1999): Cloning and characterization of two new isoforms of the rat kidney urea transporter: UT-A3 and UT-A4. J. Am. Soc. Nephrol., **10**, 230-237.

Nejsum, L.N., Elkjaer, M., Hager, H., Frokiaer, J., Kwon, T.H. and Nielsen, S. (2000): Localization of aquaporin-7 in rat and mouse kidney using RT-PCR, immunoblotting, and immunocytochemistry. Biochem. Biophys. Res. Commun., **277**, 164-170.

Schnellmann, R.G. (2001): Toxic responses of the kidney. In Casarett & Doull's Toxicology, 6th ed.(Klaassen, C.D., ed.), pp.491-514. McGraw-Hill.

Snedecor, G.W. and Cochran, W.G. (1989): Statistical Methods, 8th ed., Iowa State University Press.

Thukral, S.K., Nordone, P.J., Hu, R., Sullivan, L., Galambos, E., Fitzpatrick, V.D., Healy, L., Bass, M.B., Cosenza, M.E. and Afshari, C.A. (2005): Prediction of nephrotoxicant action and identification of candidate toxicity-related biomarkers. Toxicol. Pathol., **33**, 343-355.

Urushidani, T. and Nagao, T. (2005): Toxicogenomics: The Japanese initiative. In Handbook of Toxicogenomics - Strategies and Applications (Borlak, J., ed.), pp. 623-631. Wiley – VCH.

van de Water, B., de Graauw, M., Le Devedec, S. and Alderliesten, M. (2006): Cellular stress responses and molecular mechanisms of nephrotoxicity. Toxicol. Lett., **162**, 83-93.

Xiong, W., Chao, L. and Chao, J. (1989): Renal kallikrein mRNA localization by in situ hybridization. Kidney Int., **35**, 1324-1329.

The Journal of Toxicological Sciences,
Vol.31, No.5, 491-507, 2006

GENE EXPRESSION PROFILE IN LIVER OF DIFFERING AGES OF RATS AFTER SINGLE ORAL ADMINISTRATION OF ACETAMINOPHEN

Katsumi MORISHITA[1], Yumiko MIZUKAWA[2], Toshihiko KASAHARA[1], Manabu OKUYAMA[1], Kayoko TAKASHIMA[1], Naoki TORITSUKA[1], Toshikazu MIYAGISHIMA[1], Taku NAGAO[3] and Tetsuro URUSHIDANI[1,2]

[1]*Toxicogenomics Project, National Institute of Biomedical Innovation, 7-6-8 Saito-Asagi, Ibaraki, Osaka 567-0085, Japan*

[2]*Department of Pathophysiology, Faculty of Pharmaceutical Sciences, Doshisha Women's College of Liberal Arts, Kodo, Kyotanabe, Kyoto 610-0395, Japan*

[3]*National Institute of Health Sciences, 1-18-1 Kamiyoga, Setagaya-ku, Tokyo 158-8501, Japan*

(Received August 18, 2006; Accepted September 11, 2006)

ABSTRACT — In order to verify the influence of the rat age on hepatotoxicity, male Sprague-Dawley rats of 6 (young) and 12 (adult) weeks of age were orally administered acetaminophen (APAP), isoniazid (INH), or carbon tetrachloride (CCl4). Liver samples were obtained in a time-course manner, and changes in gene expression examined by an Affymetrix GeneChip. APAP caused more prominent hepatic injury with respect to pathology and blood biochemistry in adults than in young rats, whereas no obvious age-related differences were observed in INH- or CCl4-treated rats. Comparing gene expression in control rats, CYP3A13 was higher and GSTY2c was lower in adults, suggesting that production of the active metabolite of APAP is higher and its detoxification is lower in adults. The total amount of glutathione and total SH in rat liver was found to be higher in adult rats whereas the extent of its reduction by APAP was larger in adults. A detailed analysis of genes showing age-related differences revealed that some of them were different not in their extent but in their time course, i.e., the stress responses occurred earlier in the young than in the adult, resulting in a difference at 24 hr after dosing. These results suggest that the age-related difference in toxicity would be attributed to a higher expression of CYP3A13, producing the active metabolite of APAP as well as the lower expression of the detoxification enzyme, GSTY2c, in adult rats. Furthermore, these differences affect the time course of APAP toxicity. The present study clearly depicts the advantage of the multi-time, multi-dose protocol employed in our project for analyzing the mechanism of toxicity by gene expression profiling.

KEY WORDS: Toxicogenomics, Acetaminophen, Hepatotoxicity, Age-related difference, Rat

INTRODUCTION

The Toxicogenomics Project is a 5-year collaborative project by the National Institute of Health Sciences (NIHS) and 17 pharmaceutical companies in Japan which started in 2002 (Urushidani and Nagao, 2005). Its aim is to construct a large-scale toxicology database of transcriptome for the prediction of toxicity of new chemical entities in the early stage of drug development. About 150 chemicals, mainly medical compounds, have been selected, using both *in vitro* studies with primary hepatocyte of rat and human, and *in vivo* studies in rat. Of these, the standard protocol of *in vivo* study in TGP consists of a single administration test and a repeated administration test with multi-time and multi-dose. The gene expression of the liver is comprehensively analyzed by using Affymetrix GeneChip® with the traditional toxicity parameters. Although the ages of the rats were varied in a time-course sacrifice between 6 to 10-weeks old, we did not previously know the age-difference effect in the susceptibility of hepatotoxicity. In starting of TGP, we

Correspondence: Tetsuro URUSHIDANI (E-mail: turushid@dwc.doshisha.ac.jp)

conducted an exploratory study to clarify whether the age-related difference was present in hepatotoxicity by using the first 3 chemicals in the TGP database, i.e., APAP, isoniazid (INH), and carbon tetrachloride (CCl4). Of these 3 chemicals, APAP alone showed a significant age-related difference in hepatotoxicity. In this report, we focus on the age-difference in susceptibility of APAP hepatotoxicity and elucidate the cause of the difference.

MATERIALS AND METHODS

Chemicals

APAP, INH, and CCl4 were purchased from Sigma Co. Ltd., (St. Louis, MO). All other chemicals and reagents used in the present study were of HPLC or analytical grade and are commercially available.

Animal treatment

Male Sprague-Dawley rats were purchased from Charles River Japan Inc., (Kanagawa, Japan) at 5-weeks or 11-weeks of age. After a 7-day quarantine and acclimatization period, the animals were divided into groups of 5 using a computerized stratified random grouping method based on body weights for each age. On the administration day, the animals were 6 and 12 weeks-old, respectively. The animals were individually housed in stainless-steel cages in a room that was lighted for 12 hr (7:00-19:00) daily, ventilated with an air-exchange rate of 15 times per hour, and maintained at 21 to 25°C with a relative humidity of 40 to 70%. Each animal was allowed free access to water and pellet food (CRF-1, sterilized by radiation, OrientalYeast Co., Japan).

Five rats in each group were orally administered APAP or INH by suspending in 0.5% methylcellulose solution, and with CCl4 by dissolving in corn oil. The highest dose level for each administration was determined by a 1 week dose-finding study (data not shown) and subsequently the middle and low doses were determined, i.e., 50, 300, 1000 mg/kg for APAP, 10, 50, 200 mg/kg for INH, and 30, 100, 300 mg/kg for CCl4. Blood samples were obtained at 3, 6, 9, and 24 hr post-dose with a needle and a heparinized syringe from the abdominal artery under ether anesthesia. Plasma was obtained after centrifugation and stored below −20°C until use. Aspartate aminotansferase (AST), Alanine aminotransferase (ALT) and lactate dehydrogenase (LDH) were determined by COBAS MIRA plus autoanalyzer (Roche Diagnostics, Basel, SZ). After blood collection, the animals were euthanized by exsanguination from the abdominal veins and arteries under ether anesthesia. The liver samples were collected in 10% neutral buffered formalin at necropsy and embedded in paraffin, and then sectioned and stained with hematoxylin-eosin. Histopathological evaluation of the liver specimens was conducted by using light microscopy and graded as - (no change), +/− (minimal), + (slight), ++ (moderate), and +++ (severe).

Measurement of hepatic glutathione and SH contents

The pre-weighed (ca. 0.1 g each) liver samples were homogenized with 5% 5-sulfosalicylic acid (Sigma-Aldrich), and centrifuged at 12,000 rpm for 10 min at 4°C. The supernatant was used for measurement of total glutathione (GSH) content in liver using the Total Glutathione Quantification Kit (Dojindo Laboratories) according to the manufacturer's instructions. In this kit, GSH oxidized by DTNB is reduced by glutathione reductase; namely, an enzyme recycling method is employed. We modified this method in order to measure the total free SH contents in the sample. In brief, the manufacturer's instructions were followed except that the glutathione reductase solution was replaced with a buffer solution and the dilution factor for the sample and GSH standard solutions was reduced ca. 1/5 − 1/10 fold. The reaction time was 10 min at room temperature and the measurement was done by a pseudo-end point method. The results were expressed as SH equivalent to the standard GSH per wet weight (g) in both measurements.

Microarray experiment

An aliquot of the sample (about 30 mg) was obtained from the left lateral lobe of the liver of each animal immediately after sacrifice, and put into RNA later® (Ambion, Austin, TX, USA) overnight for 4°C and then frozen. Homogenization was conducted by Mill Mixer (Qiagen) and zirconium beads. The purity of the RNA was checked by gel electrophoresis, and the 260/280 nm ratio was between 2.0-2.2. Total RNA was isolated using RNeasy kit by Bio Robot 3000 (Qiagen, Valencia, CA, USA).

Microarray analysis was conducted on 3 out of 5 samples for each group by using GeneChip® RAE230A probe arrays (Affymetrix, Santa Clara, CA, USA) containing 15923 probe sets. The procedure was conducted basically according to the manufacturer's instructions. Briefly, 5 μg of total RNA was used for the synthesis of cDNA with the Superscript Choice

System (Invitrogen, Carlsbad, CA, USA) and T7-$(dT)_{24}$-oligonucleotide primer (Affymetrix). After the cDNA was purified by cDNA Cleanup Module (Affymetrix), biotin-labeled cRNA was synthesized by using the BioArray High yield RNA Transcript Labeling Kit (Enzo Diagnostics, Farmingdale, NY, USA). The cRNA was purified by an IVT cRNA Cleanup Spin Column (Affymetrix), and then fragmented. Twenty μg of the fragmented cRNA was hybridized to a RAE230A probe array for 18 hr at 45°C at 60 rpm. After hybridization, the array was washed and stained by streptavidin-phycoerythrin using the Fluidics Station 400 (Affymetrix). Finally, the array was scanned by Gene Array Scanner (Affymetrix). The digital image files were processed by Affymetrix Microarray Suite version 5.0.

Statistical analysis

The data from biochemistry was expressed as the mean value of the 5 animals in each group. In the present experiments, the data of blood biochemistry showed large variations and we thus employed Mann-Whitney's U-test (Snedecor and Cochran, 1989) for analyzing the drug effects.

Gene expression data were analyzed by using GeneSpring® version 6.1 (Silicon Genetics, Santa Clara, CA, USA). Expression data was normalized by the mean value (global normalization; adjusted to an arbitrary value of 500). After filtering the genes by flags (present or marginal call at least 12 of the 24 samples in each experiment), the fold change determination to the concurrent control samples was performed in order to extract drug-related changes. In some cases, Student's *t*-test (Snedecor and Cochran, 1989) with Benjamin's adjustment ($p<0.05$) was also used for the age-difference comparison using the control samples.

RESULTS

Phenotype change by APAP, INH and CCl4

Time-course changes in plasma AST, ALT and LDH after administrations of APAP, INH, and CCl4 are shown in Table 1. In APAP-treated rats, significant increases of ALT and AST were noted in adult rats at 24 hr after treatment of 1000 mg/kg. Young rats treated with the same dosage showed a tendency of increment of these enzyme activities, but it was not statistically significant. In the cases of INH and CCl4, no obvious increase of these enzymes was detected. Although a significant statistical difference in young rats was detected 9 hr after INH-treatment, it was a decrease in the measure and thus considered not to be toxic.

Histopathological findings of the liver are shown in Table 2. At 24 hr post-dose of APAP, necrosis, increased eosinophility and vacuolation of hepatocyte were observed with inflammatory cells infiltration at 1000 mg/kg in both ages. Of these, hepatocyte necrosis in adult rats was more evident than that in young rats. In the young rats, minimal necrosis (grade +/–) was only noted in 2 out of 5 animals (Photo 1A), whereas all of the adult rats had necrosis: 2 of them were grade + (Photo 1B) and the remaining 3 were grade +/–.

No obvious changes were found in the liver with this dose range of INH. Although CCl4 caused some pathological changes in the liver, no obvious age-related differences were noted. Both biochemistry and histopathology indicated that hepatotoxicity of APAP was evident, i.e., increases in the leak of the enzymes and centrilobular necrosis of hepatocytes, and adult rats appeared to be more susceptible to hepatotoxicity than the young ones.

Age-dependent gene expression

Based on the biochemical and histopathological data, the age-related difference appeared to be specific for APAP among the three chemicals. This suggested that there should be some difference in the factors specifically involved in APAP-induced hepatotoxicity. In order to elucidate the cause of the difference, we tried to extract genes with different expression by age from control animals.

Nine control animals in each time point were employed for both young and adult rats from the TGP database, and the genes that changed more than 2-fold between the ages with statistical significance ($p < 0.05$) in all time points (3, 6, 9, and 24 hr) were extracted (Table 3). Of the total 11 genes extracted, 7 genes were lower and 4 genes were higher in adult rats than in young ones. They contained "hemoglobin beta chain complex" and "aminolevulinic acid synthase 2" (the rate-limiting enzyme in hepatic porphyrin-heme biosynthesis), both of which appeared to reflect the biosynthesis of red blood cells in the liver, and this appears to be reasonable, because extramedullary hematopoiesis decreases with age. As for changes related to APAP toxicity, it was noteworthy that the lower value of glutathione *S*-transferase Yc2 (GSTYc2) and the higher value of Cyp3A13 in adult rats were clearly indicated. Fig.1 shows the time- and dose-dependent effects of APAP on the expression of these two genes. GSTYc2 (Fig. 1A) was found to be always higher in young than in adult rats. Nine hr after

Table 1. Changes in Blood biochemistry after treatment with 1000 mg/kg of Acetaminophen (APAP), 200 mg/kg of Isoniazid (INH) and 300 mg/kg carbon tetrachloride (CCl4).

Compound	Age (week)	Dose (mg/kg)	Time (hr)	Number of Amimals	AST (IU/L)	ALT (IU/L)	LDH (IU/L)
APAP	6	0	3	5	66.2 ± 9.6	35.0 ± 8.7	111.2 ± 47.3
			6	5	63.4 ± 7.8	32.2 ± 4.1	105.2 ± 32.0
			9	5	53.4 ± 4.2	28.6 ± 3.4	81.6 ± 24.0
			24	5	59.0 ± 6.3	37.0 ± 3.1	105.2 ± 33.8
		1000	3	5	66.2 ± 7.3	36.8 ± 5.2	88.2 ± 14.2
			6	5	61.8 ± 4.2	31.2 ± 1.8	119.2 ± 21.4
			9	5	60.2 ± 4.1	30.8 ± 5.9	107.2 ± 30.1
			24	5	76.4 ± 14.1	51.0 ± 17.2	134.4 ± 31.9
	12	0	3	5	68.4 ± 17.1	29.2 ± 5.4	115.6 ± 29.8
			6	5	56.6 ± 7.3	25.0 ± 2.5	122.6 ± 44.9
			9	5	52.6 ± 2.2	25.2 ± 2.2	100.8 ± 54.6
			24	5	65.6 ± 12.5	29.8 ± 5.3	122.8 ± 62.1
		1000	3	5	63.4 ± 11.1	30.8 ± 7.7	109.2 ± 24.7
			6	5	58.6 ± 3.0	26.6 ± 3.8	93.0 ± 15.0
			9	5	52.0 ± 3.7	26.4 ± 4.7	121.8 ± 62.2
			24	5	287.8 ± 221.0 *	78.4 ± 62.3 *	315.4 ± 208.1
INAH	6	0	3	5	59.8 ± 7.2	34.0 ± 4.5	92.0 ± 19.8
			6	5	55.2 ± 7.2	26.8 ± 4.9	114.2 ± 36.1
			9	5	55.4 ± 5.0 *	27.4 ± 2.3	82.6 ± 29.5
			24	5	59.6 ± 8.2	33.2 ± 4.7	109.4 ± 46.5
		200	3	5	58.2 ± 5.8	31.4 ± 3.6	86.6 ± 22.9
			6	5	50.0 ± 2.2	24.0 ± 2.0	92.0 ± 16.2
			9	5	39.2 ± 6.7	24.6 ± 1.3	94.6 ± 26.1
			24	5	47.6 ± 6.7	21.2 ± 6.6	96.0 ± 25.6
	12	0	3	5	54.8 ± 10.5	25.0 ± 7.6	93.4 ± 44.9
			6	5	49.8 ± 11.7	24.2 ± 3.6	87.0 ± 38.6
			9	5	46.0 ± 16.2	22.6 ± 4.4	112.0 ± 85.9
			24	5	50.8 ± 9.1	26.6 ± 9.7	99.0 ± 30.6
		200	3	5	51.2 ± 10.8	27.2 ± 4.0	85.2 ± 34.6
			6	5	42.4 ± 3.6	22.4 ± 3.9	77.0 ± 29.2
			9	5	29.0 ± 7.1	19.2 ± 4.9	83.0 ± 30.4
			24	5	41.4 ± 11.0	14.2 ± 4.1	89.8 ± 41.2
CCl4	6	0	3	5	66.6 ± 2.7	37.2 ± 7.2	209.0 ± 109.8
			6	5	62.8 ± 5.1	31.4 ± 2.1	189.2 ± 78.5
			9	5	62.6 ± 9.9	30.0 ± 4.2	163.0 ± 55.4
			24	5	66.6 ± 4.0	37.2 ± 2.7	186.2 ± 67.2
		300	3	5	67.8 ± 4.3	39.4 ± 4.5	201.4 ± 74.9
			6	5	65.2 ± 5.7	29.8 ± 4.6	205.8 ± 48.3
			9	5	63.2 ± 5.8	28.4 ± 1.5	200.2 ± 59.1
			24	5	75.0 ± 13.3	42.2 ± 4.6	192.6 ± 38.2
	12	0	3	5	73.0 ± 18.8	37.8 ± 7.6	156.6 ± 30.4
			6	5	90.6 ± 38.4	47.6 ± 25.2	181.2 ± 32.5
			9	5	131.8 ± 162.9	123.2 ± 206.7	239.6 ± 100.7
			24	5	63.4 ± 10.6	34.6 ± 4.0	171.6 ± 51.0
		300	3	5	65.6 ± 9.9	35.6 ± 5.7	213.2 ± 58.6
			6	5	75.4 ± 21.1	37.0 ± 16.5	179.2 ± 71.4
			9	5	72.6 ± 17.8	31.4 ± 10.7	235.8 ± 110.0
			24	5	68.8 ± 1.5	36.6 ± 4.1	201.8 ± 60.6

Data are expressed as mean ± SD of 5 measurements. * $p<0.05$; significantly different from control by Mann-Whitney's U-test.

dosing, APAP clearly up-regulated the expression of the enzyme and the values after the induction were still higher in young than adult rats. In the case of CYP3A13, its expression was always lower in young than in adult rats and was not affected by APAP at all (Fig. 1B).

In order not to miss other molecular species, the expressions of CYP and GST were checked. There are

Table 2. Histopathological changes of liver by 1000 mg/kg of acetaminophen (APAP), 200 mg/kg of isoniazid (INH) and 300 mg/kg of carbon tetrachloride (CCl4).

Compound	Age (Week)	Time (hr)	Findings	Number of animals							
				Control				High dose			
			Grade	−	±	+	++	−	±	+	++
APAP	6	3	No abnormal findings								
		6	No abnormal findings								
		9	Increased eosinophility of hepatocyte	5				2	3		
		24	Necrosis of hepatocyte	5				3	2		
			Increased eosinophility of hepatocyte	5					1	2	2
			Vacuolar change of hepatocyte	5				4		1	
			Inflammatory infiltration	5					1	4	
	12	3	No abnormal findings								
		6	No abnormal findings								
		9	No abnormal findings								
		24	Necrosis of hepatocyte	5					3	2	
			Increased eosinophility of hepatocyte	5						2	3
			Vacuolar change of hepatocyte	5				4	1		
			Inflammatory infiltration	5					2	3	
INAH	6	3	No abnormal findings								
		6	No abnormal findings								
		9	No abnormal findings								
		24	No abnormal findings								
	12	3	No abnormal findings								
		6	No abnormal findings								
		9	No abnormal findings								
		24	No abnormal findings								
CCl4	6	3	Degeneration, hydropic	5				2	2	1	
		6	Degeneration, hydropic	5				1	2	2	
			Cellular infiltration	5				4	1		
		9	Degeneration, hydropic	5				1	4		
			Cellular infiltration	5				4	1		
		24	Degeneration, hydropic	5				1	4		
			Cellular infiltration	5				2	3		
			Degeneration, fatty	5					1	4	
	12	3	Degeneration, hydropic	5				2	2	1	
		6	Degeneration, hydropic	5				2	3		
			Cellular infiltration	5					5		
		9	Degeneration, hydropic	5				2	3		
			Cellular infiltration	5				1	4		
		24	Degeneration, hydropic	5				3	2		
			Cellular infiltration	5					5		
			Degeneration, fatty	5					2	3	

Grade indication: no change (−), minimal (±), slight (+), moderate (++).

Table 3. Differentially expressed genes in control animals between 6 and 12 week-old rats.

Probe Set ID	Gene ID	Gene Symbol	Fold change v.s. 6W				P-value				Gene Title
			3H	6H	9H	24H	3H	6H	9H	24H	
1387123_at	NM_012753	Cyp17a1	0.23	0.34	0.26	0.24	3.9E-04	4.1E-02	1.6E-03	1.9E-03	cytochrome P450, family 17, subfamily a, polypeptide 1
1371089_at	AA945082	Yc2	0.21	0.28	0.15	0.30	2.4E-04	7.0E-03	3.5E-03	8.6E-03	glutathione *S*-transferase Yc2 subunit
1368160_at	NM_013144	Igfbp1	0.23	0.14	0.23	0.33	1.4E-03	2.0E-03	4.7E-02	2.8E-02	insulin-like growth factor binding protein 1
1371102_x_at	X05080	Hbb	0.42	0.43	0.27	0.35	9.4E-03	2.0E-03	7.9E-05	3.1E-03	hemoglobin beta chain complex
1371245_a_at	BI287300	---	0.45	0.39	0.24	0.38	1.4E-02	9.4E-04	3.4E-05	2.5E-03	---
1367985_at	NM_013197	Alas2	0.42	0.41	0.32	0.42	7.0E-04	4.6E-03	2.5E-05	1.4E-03	aminolevulinic acid synthase 2
1387022_at	NM_022407	Aldh1a1	0.42	0.41	0.35	0.44	3.5E-03	1.2E-02	3.5E-03	1.1E-02	aldehyde dehydrogenase family 1, member A1
1369465_at	NM_012584	Hsd3b	2.6	2.4	2.7	2.0	1.9E-03	2.9E-02	1.7E-03	3.1E-02	steroid delta-isomerase, 3 beta
1390146_at	BF414998	RGD1306105_predicted	2.5	3.4	3.1	2.9	2.0E-03	1.6E-03	1.7E-03	1.1E-03	similar to RIKEN cDNA 2610318G18 (predicted)
1370387_at	U46118	Cyp3a13	6.4	5.1	4.7	3.4	1.4E-03	1.3E-02	3.0E-04	1.4E-03	cytochrome P450, family 3, subfamily a, polypeptide 13
1368171_at	NM_017061	Lox	2.7	5.6	7.4	3.6	1.9E-02	2.5E-02	7.9E-05	2.7E-02	lysyl oxidase

Nine control animals for each time point were employed for both young and adult rats from the TGP database, and the genes that changed more than 2-fold between the ages with statistical significance ($p < 0.05$, Student's *t*-test with Benjamin's adjustment) in all time points (3, 6, 9, and 24 hr) were extracted. Fold changes of 12-week vs. 6-week and their p values at each time point are also shown.

19 probe sets annotated with GST, while GSTYc2 was the only one with a difference between young and adult. A comparison between young and adult rats was made at 24 hr after the treatment with 1000 mg/kg of APAP and significant differences were detected in three GSTs, i.e., GST mu 2, microsomal GST 3 (predicted), and GST omega, all of which showed lower values in adult than in young rats (data not shown). There are 63 probe sets annotated with CYP, and only CYP17A1 and CYP2C40 (in addition to CYP3A13) were found to be differentially expressed between young and adult rats, and the former two had much lower values in adult than in young rats. No probe sets with different sensitivity to APAP treatment between ages were detected in CYPs. As CYP17A1 and CYP2C40 are involved in steroid biosynthesis and arachidonic acid metabolism, respectively, CYP3A13 was found to be the only candidate for CYP with age-related difference that produces active metabolites of APAP.

The above results could explain the observation that adult rats showed high sensitivity to APAP. In order to explain the specificity of the chemicals, we checked the expressions of CYP2E1 and *N*-acetyltransferase, which are considered to be involved in production of active metabolites of INH and/or CCl4. As described above, CYP2E1 had no age-related difference, and this was the same for the INH- or CCl4-treated group. There are 6 probe sets annotated with *N*-acetyltransferase, and none of them showed significant age-related differences regardless of treatment with INH (data not shown).

Measurement of GSH and SH

It is a consensus that APAP is converted into an active metabolite that is detoxified by GSH conjugation and hepatotoxicity emerges when intracellular GSH is depleted. From the present results, it was suggested that adult rats had a high ability to produce the active metabolite but low capacity of detoxification and that subsequently this caused GSH-depletion more easily as compared with young rats. This was confirmed by direct measurements of hepatic GSH and SH contents by the DTNB method. The results are shown in Fig. 2. Both GSH and free SH contents per wet weight of liver in adult rats showed a value twice as high as that in young rats. Twenty-four hr after treatment with 1000 mg/kg of APAP, these measures did not change in young rats, whereas they showed a remarkable decrease in adults with a statistical significance in free SH contents. This supported our assumption that the high sensitivity to APAP in adult rats is attributed to the high degree of GSH-depletion.

Gene expression changes by APAP

Numbers of altered genes with 2-fold or more of

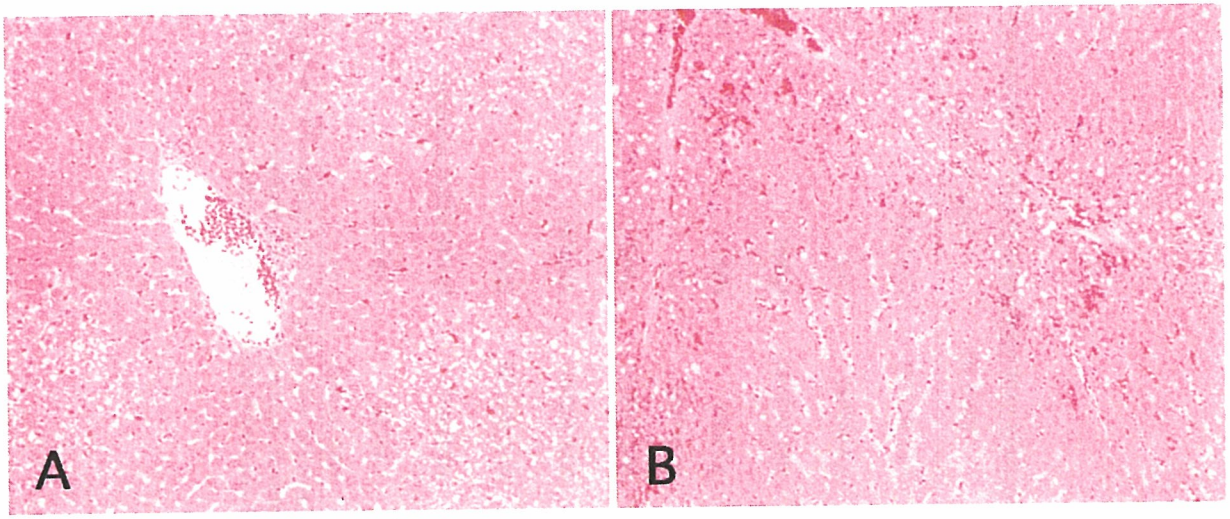

Photo 1. H&E-stained sections of rat liver 24 hr after oral administration of 1000 mg/kg APAP. A: 6-week-old rat; centrilobular necrosis +/–, eosinophility ++, inflammatory infiltration +. B: 12-week-old rat; centrilobular necrosis +, eosinophility ++, inflammatory infiltration +.

the corresponding control in the highest doses of APAP, INH, and CCl4 are shown in Table 4. In this analysis, we did not use statistical filtering because we considered that it was favorable to overview the drug-related changes in order to compare the age difference between young and adult rats. The numbers of genes affected by APAP were greater in adult rats than those in young rats for all time points. In contrast, INH and CCl4 did not show any clear tendency in terms of the age-related difference in the numbers of mobilized genes.

The altered genes with more than 3-fold change vs. control at 24 hr post-dose of APAP in adult rats are listed in Table 5 (up-regulated genes), and those with less than 1/3 vs. control at 24 hr in adult rats are listed in Table 6 (down-regulated genes). The fold change of

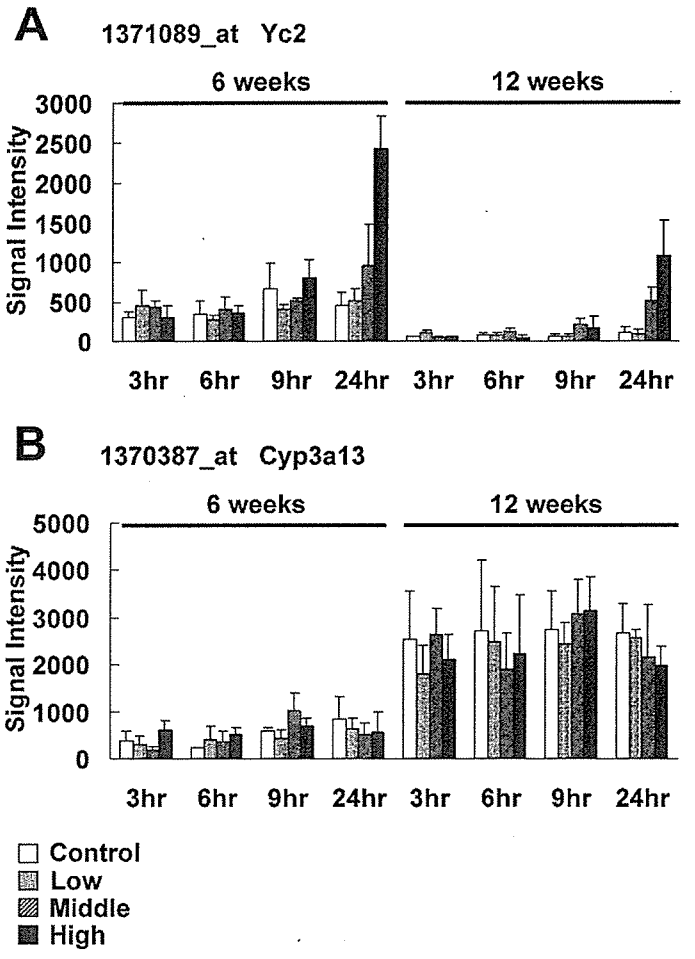

Fig. 1. Time- and dose-dependent effects of APAP on the expression of glutathione *S*-transferase Yc2 (1371089_at) and Cyp3a13 (1370387_at). Rats 6- or 12-week-old were treated with 50 (low), 300 (middle) and 1000 (high) mg/kg of APAP and sacrificed at 3, 6, 9, and 24 hr after treatment. Gene expression in liver was analyzed by using GeneChip® RAE230A probe arrays and the signals obtained by Affymetrix Microarray Suite version 5.0 were normalized by using the mean value of each chip adjusted to an arbitrary value of 500 and expressed as mean ± SD (N=3).

each gene in young rats is also included in these tables. Response to oxidative stress (Hspla, Hsplb, Hmox1, Txnrd1, Hspb8, Hspca, Hspb8), glutathione metabolism (Gss, Gstp, Gsr, Gclc), and response to DNA damage (Ddit4, Prp19, Apex1, Gadd45a) were up-regulated in adult rats. Cell proliferation (pcna, Nap111, Gnl3), part of glutathione metabolism (Gsr, Gclc), UDP-glucuronocyltransferase (RGD:708541, RGD:708417) were up-regulated in both young and adult rats. However, microsomal enzymes (Cyp7A1, Cyp3A11, Cyp17A1, Comt, Gulo, G6pc, Sec11, RGD:2467, G6pc, Fmo1, Gulo) and mitochondrial enzymes (Glul, Oat, Ehhadh, Abcc8, Otc, Abat, Ivd, Abcc9, Aadat, Ca5a, Acsl1) were dominantly down-regulated in adult rats. Of these, some mitochondrial enzymes (Oat, Ehhadh and Ivd) were also down-regulated in young rats. These results indicated that the gene expression changes in adult rats were also greater than those in young ones, reflecting the degree of liver damage.

Changes of some representative genes are depicted as Fig. 3 and Fig. 4, which show time- and dose-dependency. In genes such as Egr1, Dnajb1 (predicted), Ddit3, and Hspca (Fig. 3A-D), their expression was highly up-regulated 24 hr after treatment of the highest dose and the extent of induction was remarkably different between ages. On the other hand, in the genes such as Hsp a1a, Hmox-1, Gadd45, and Txnrd (Fig. 4A-D), their induction was larger in adult than young 24 hr after treatment, whereas induction in the young ones occurred at an earlier time point than the adults, i.e., the extent of induction of these genes were much higher in the young than in the adult at early time points. Namely, part of the protective response against APAP started earlier in young rats.

By analyzing the time- and dose-dependent manner, it was revealed that some of stress-related genes responded faster in young than adult rats by APAP. Since expression of these genes was not affected by INH or CCl4, it was not a feature of young rats but rather specific for APAP among these chemicals. Furthermore, reviewing the histopathology in Table 2, cell infiltration with minimal extent occurred at 9 hr only in the young rats, supporting the result of the above gene expression analysis.

DISCUSSION

The mechanism of hepatotoxicity by APAP has been proposed in some papers (Cohen and Khairallah, 1997; Parkinson, 2001; Bessems and Vermeulen, 2001; Irwin *et al.*, 2004). The most widely accepted mecha-

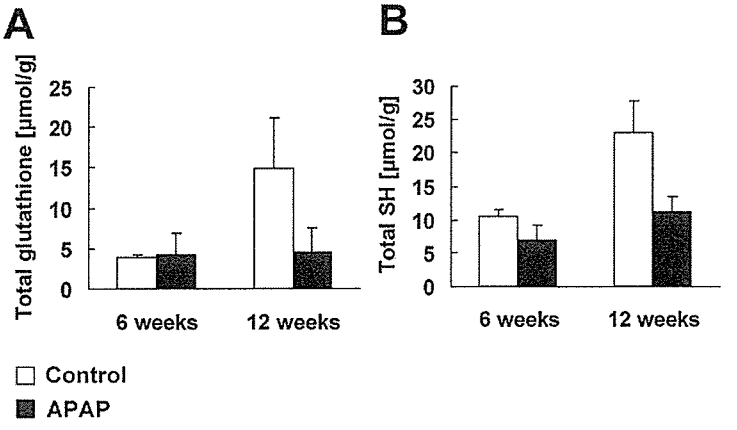

Fig. 2. Effects of APAP on hepatic content of total glutathione and SH of 6- and 12 week-old rats.
Both 6- or 12-week-old rats received 1000 mg/kg APAP orally and liver samples obtained 24 hr later. A: total glutathione contents expressed as µmol glutathione per g wet weight, B: total SH contents equivalent to µmol glutathione per g wet weight. Values are mean ± SD (N=3). A statistically significant reduction of total SH was observed in 12-week rats ($p<0.05$).

nism is that APAP is biotransformed to a reactive intermediate (*N*-acetyl-*p*-benzoquinone imine) by cytochrome P450s (Cyp2E1 and Cyp3A) in liver. The main detoxification pathway is considered to be GSH-conjugation. Finally, overflow of intermediate and/or depletion of GSH cause protein arylation and/or oxidation, and subsequently leads to necrosis of the liver. Expression changes by APAP in the present study were generally in agreement with the above mechanism of action, i.e., response to oxidative stress, glutathione metabolism, response to DNA damage, cell proliferation, and conjugation enzymes were up-regulated and several microsomal enzymes and mitochondrial enzymes were down-regulated. Of these, down-regulation of several microsomal enzymes and mitochondrial enzymes could be explained by the organelle function, because the microsome was the place where the reactive metabolite was produced and cell death was closely related to mitochondrial damage (Jaeschke and Bajt, 2006). These changes by APAP were also greater in adult rats than in young rats at 24 hr after dosing.

Table 4. Number of genes whose expression was changed more than 2-fold by 1000 mg/kg of APAP, 200 mg/kg of INH or 300 mg/kg of CCl4.

Compound	Age (week)	Time (hr)	Number of Genes	
			Increased	Decreased
APAP	6	3	27	67
		6	14	32
		9	19	39
		24	137	149
	12	3	32	88
		6	33	198
		9	34	67
		24	220	193
INAH	6	3	15	17
		6	6	13
		9	5	25
		24	3	34
	12	3	4	15
		6	1	20
		9	18	19
		24	6	62
CCl4	6	3	15	25
		6	10	73
		9	5	31
		24	21	39
	12	3	34	24
		6	4	24
		9	14	12
		24	9	64

Expression data was normalized by mean value (global normalization; adjusted to an arbitrary value of 500) and filtering of the genes by flags (present or marginal call at least 12 of the 24 samples in each experiment) was performed. The fold change of each of the probe sets by the drug was calculated and the numbers of the genes showing more than 2-fold or less than half of control value were counted for each age.

Although there have been several studies where hepatotoxicity of APAP in rodent was analyzed by gene expression (Reilly *et al.*, 2001; Ruepp *et al.*, 2002; Irwin *et al.*, 2004; Heinloth *et al.*, 2004), there is a limited number of papers regarding the age difference in the susceptibility of hepatotoxicity. A few papers described age-related differences such as weanling vs. mature (Allameh *et al.*, 1997), 11-day vs. 33-day-old (Green *et al.*, 1984), or 4-month vs. 25-month-old rats (Rikans and Moore, 1988), but the cause of the differences was not well clarified (Rikans, 1989; Tarloff *et al.*, 1996). There was no information about the difference in susceptibility concerning young to mature age, either. As 6 week-old rats are generally used for toxicological tests (and thus we employ this age for creating our toxicogenomics database), we are interested in the sensitivity of rats of this age against hepatotoxicants compared with matured rats, such as 12-week-olds.

In the present study, a single oral dose of APAP at 1000 mg/kg caused marginal hepatotoxicity in young rats, such as a tendency for an increase in plasma enzymes and minimal hepatocyte necrosis. Under the same condition, adult rats showed more prominent toxicity. This age-related difference should be based on APAP-specific mechanism(s), since no age-related differences were noted in INH or CCl4-induced hepatotoxicity. From the present results and literatures, the main mechanism was considered to be as follows: a) the expression of CYP3A13 that produces the active metabolite of APAP is higher in adult than in young rats, b) among the GST species that detoxify the active metabolite of APAP, the expression of GSTYc2 is lower in adult than in young, and c) the expression of GST, mu 2, microsomal GST 3 (predicted), GST omega 1 are inhibited by APAP.

The modification of APAP toxicity by modifying Cyp3A has been reported in rodents. Inhibition of Cyp3A prevented APAP hepatotoxicity (Kostrubsky *et al.*, 1997), whereas caffeine, dexamethazone, troglitazone or pregnenolone 16 alpha-carbonitrile, all of

Table 5. List of genes that showed expression of more than 3-fold of control by APAP at 24 hr at 12-week-old rats.

Probe Set ID	Gene Symbol	Gene ID	Fold change 6W	Fold change 12W	Gene Title
1368247_at	Hspa1a /// Hspa1b_mapped	NM_031971		37.3	heat shock 70kD protein 1A /// heat shock 70kD protein 1B (mapped)
1370912_at	Hspa1b_mapped	BI278231		30.0	heat shock 70kD protein 1B (mapped)
1368321_at	Egr1	NM_012551		17.3	early growth response 1
1372510_at	Srxn1	AI172302	2.7	17.0	Sulfiredoxin 1 homolog (S. cerevisiae)
1383302_at	Dnajb1_predicted	BM384926		12.4	DnaJ (Hsp40) homolog, subfamily B, member 1 (predicted)
1387060_at	Klf6	NM_031642		10.1	Kruppel-like factor 6
1370080_at	Hmox1	NM_012580		9.3	heme oxygenase (decycling) 1
1368160_at	Igfbp1	NM_013144	4.0	8.8	insulin-like growth factor binding protein 1
1370436_at	LOC246263	AF062389	3.1	8.4	kidney-specific protein (KS)
1386321_s_at	Trib3	H31287	3.9	7.9	tribbles homolog 3 (Drosophila)
1388986_at	---	AI598339		7.8	Transcribed locus
1367856_at	G6pdx	NM_017006	2.9	7.8	glucose-6-phosphate dehydrogenase X-linked
1389528_s_at	Jun	BI288619		7.7	Jun oncogene
1367795_at	Ifrd1	NM_019242		7.4	interferon-related developmental regulator 1
1388271_at	---	BM383531	4.4	7.3	---
1374404_at	Jun	BI288619		6.9	Jun oncogene
1388722_at	Dnajb1_predicted	AA945704		6.8	DnaJ (Hsp40) homolog, subfamily B, member 1 (predicted)
1368308_at	Myc	NM_012603		6.4	myelocytomatosis viral oncogene homolog (avian)
1368947_at	Gadd45a	NM_024127		6.4	growth arrest and DNA-damage-inducible 45 alpha
1386958_at	Txnrd1	U63923		6.4	thioredoxin reductase 1
1368121_at	Akr7a3	NM_013215	5.2	6.3	aldo-keto reductase family 7, member A3 (aflatoxin aldehyde reductase)
1368718_at	Aldh1a4	M23995		6.2	aldehyde dehydrogenase family 1, subfamily A4
1370688_at	Gclc	J05181	2.7	5.9	glutamate-cysteine ligase, catalytic subunit
1375852_at	Hmgcr	BM390399		5.9	3-hydroxy-3-methylglutaryl-Coenzyme A reductase
1371785_at	Tnfrsf12a	BI303379		5.3	tumor necrosis factor receptor superfamily, member 12a
1368124_at	Dusp5	NM_133578		5.3	dual specificity phosphatase 5
1398343_at	Dnaja4	AI104324		5.0	DnaJ (Hsp40) homolog, subfamily A, member 4
1374433_at	RGD1563902_predicted	BI301532		4.9	Similar to Ferritin light chain (Ferritin L subunit) (predicted)
1369590_a_at	Ddit3	NM_024134		4.7	DNA-damage inducible transcript 3
1398791_at	Txnrd1	NM_031614		4.6	thioredoxin reductase 1
1387282_at	Hspb8	NM_053612		4.5	heat shock 22kDa protein 8
1387599_a_at	Nqo1	J02679	4.2	4.5	NAD(P)H dehydrogenase, quinone 1
1387022_at	Aldh1a1	NM_022407	2.2	4.5	aldehyde dehydrogenase family 1, member A1
1390026_at	Bag3	AI231792		4.3	Bcl2-associated athanogene 3
1370030_at	Gclm	NM_017305	4.4	4.3	glutamate cysteine ligase, modifier subunit
1388850_at	Hspca	BG671521		4.3	heat shock protein 1, alpha
1388898_at	Hsph1	AI236601		4.2	heat shock 105kDa/110kDa protein 1
1384427_at	Mdm2_predicted	BI296301		4.2	transformed mouse 3T3 cell double minute 2 homolog (mouse) (predicted)